Report for 2004OR47B: Synergetic effects of colloids and organic matter on membrane fouling

There are no reported publications resulting from this project.

Report Follows

Start Date: 3/1/2004 **End Date**: 3/28/2005

Title: Combined Fouling and Chemical Cleaning of Nanofiltration Membranes

Focus Category: Water Use, Water Treatment and Water Quality

Principle Investigator: Qilin Li

Congressional District: Oregon 5

Abstract

This project was conducted to determine the synergetic effect of combined fouling of nanofiltration (NF) membranes by colloidal material and dissolved organic matter in drinking water purification, to reveal the mechanisms of combined fouling, and to develop efficient chemical cleaning strategies for membrane flux recovery. Nanofiltration experiments were conducted using synthetic waters that simulate different drinking water qualities, and the combined colloid/organic fouling layer formed was analyzed using microscopic techniques to determine the roles of colloidal material and dissolved organic matter in combined fouling under various solution chemistries. These results revealed that deposition of colloids and dissolved organic matter was drastically enhanced by the interactions between colloidal material and organic matter, leading to greater membrane flux decline. However, the combined fouling layer could be easily removed by hydraulic flushing due to the lack of specific interactions among foulants, which was found in organic fouling.

Problem and Research Objectives

Water shortage and drinking water safety are two critical issues worldwide. With population growth, industrial development, and natural water source contamination, these problems are becoming more and more serious.

Today, the American West is the fastest growing region of the country. However, water, which plays a pivotal role in this region, is the scarcest resource. In some areas, the water supply is not or will not be adequate to meet all demands of water even in normal water years. Water crisis is magnified when severe droughts are encountered. To alleviate the water shortage problem, alternative water sources − wastewater, salty water and other impaired water − are considered. These waters can be purified to meet water quality standards for direct and indirect water reuse using advanced technology such as nanofiltration (NF) and reverse osmosis (RO).

In addition to quantity, water quality is another issue of great concern. Conventional drinking water treatment processes are no longer able to meet the standards for all regulated contaminants, examples of which include synthetic organic compounds and disinfection by-products. Also, poor removal efficiency of dissolved organic carbon (DOC) by conventional treatment processes results in product water that is not biologically stable. Advanced treatment by membrane filtration, such as NF and RO, offers an almost absolute barrier to inorganic, organic and microbial contaminants.

The major obstacle for efficient applications of NF and RO membrane technology in drinking water purification, desalination and wastewater reclamation is membrane fouling.

Membrane fouling results in deterioration of membrane performance (*i.e.*, permeate flux and quality) and ultimately shortens membrane life. However, our understanding of membrane fouling is very limited and the fouling problem is far from being solved. It is necessary to understand the mechanisms of membrane fouling so that further research can be directed towards developing low-fouling membrane materials and optimizing membrane filtration systems. Despite the vast efforts to reduce membrane fouling — by improving membrane surface properties, optimizing operational conditions, or pretreatment of feed water — fouling is still inevitable. Thus, it is imperative to develop efficient chemical cleaning agents and procedures for routine cleaning of fouled membranes.

The objectives of this project are: (1) to determine the synergetic effect of combined fouling of nanofiltration (NF) membranes by colloidal material and dissolved organic matter; (2) to reveal the mechanisms of combined fouling, and (3) to develop efficient chemical cleaning strategies for membrane flux recovery.

Methods, Procedures, and Facilities

General approach. Both microscopic characterization of the fouling layer and bench-scale membrane filtration/chemical cleaning experiments were performed to determine the effect of colloidal material and dissolved organic matter in combined fouling and membrane chemical cleaning. The mechanisms of combined fouling were investigated by relating the fouling layer characteristics, which controls the mass transfer resistance of the fouled membrane and the rate of membrane flux decline, to the colloidal/organic composition of the feed water. The mechanisms of chemical cleaning were determined from changes in the fouling layer characteristics.

Model Membrane, feed water and chemical cleaning agents. A thin-film composite nanofiltration membrane, NF-270 (FilmTec Corp., Minneapolis, MN), was tested. The surface morphology of the membrane was analyzed using a Multimode atomic force microscope (AFM) (Digital Instruments, Santa Barbara, CA), and zeta potential of the membrane surface was determined by streaming potential measurements conducted with an electrokinetic analyzer (BI-EKA, Brookhaven Instruments Corp., Holtsville, NY) [1,2].

Synthetic waters were formulated using an organic model foulants, Suwannee River humic acid (SRHA) standard (International Humic Substances Society, St. Paul, MN), two model silica colloids with different particle sizes: MP3040 (300 nm) and ST-XL (30-40 nm) (Nissan Chemicals, Westheimer, TX), and typical simple electrolyte found in surface water. Deionized water, NaOH (pH 11), sodium ethylenediaminetetraacetate (EDTA), and sodium dodecyl sulfate (SDS) (Fisher Scientific, Pittsburgh, PA) were used as the model chemical cleaning agents. These chemical agents are common ingredients in commercial chemical cleaning solutions for organic-fouled membranes [3].

Filtration test units. Fouling experiments were conducted in both dead-end mode and cross-flow mode. The schematics of the two filtration systems are shown in Figures 1 and 2. The dead-end filtration unit comprises a stainless steel stirred cell modified from a commercial product (Millipore Corporation, Bedford, MA). The capacity of the cell is 400 mL and it houses a 76 mm diameter membrane sample. Three stainless steel reservoirs hold deionized water, electrolyte solution and the feed foulant solution, respectively, which are used in different stages of the fouling experiment. Pressure, provided by a compressed high purity N_2 tank, can be applied to any of the feed reservoirs or directly to the stirred cell via a 5-port valve. Membrane permeate is collected and the mass is monitored continuously by an analytical balance connected

to a lab PC to calculate the permeate flux. In the cross-flow system, the feed solution is kept in a temperature-controlled reservoir under constant mixing. It is fed to the custom-made filtration unit by a high pressure pump. The flow rate and hence cross-flow velocity are controlled by a by-pass valve and the transmembrane pressure is regulated by a backpressure regulator (GO Regulator, Inc., Spartanburg, SC). In order to avoid concentration of organics in the system, both the retentate and the permeate are recirculated to the feed reservoir. Membrane permeate flux is measured by a digital flow meter (Agilent, Palo Alto, CA) connected to a lab PC.

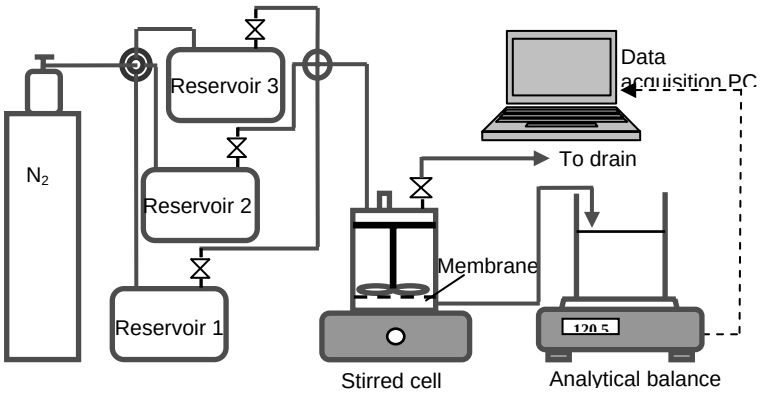

Figure 1. Schematic of the dead-end membrane filtration system

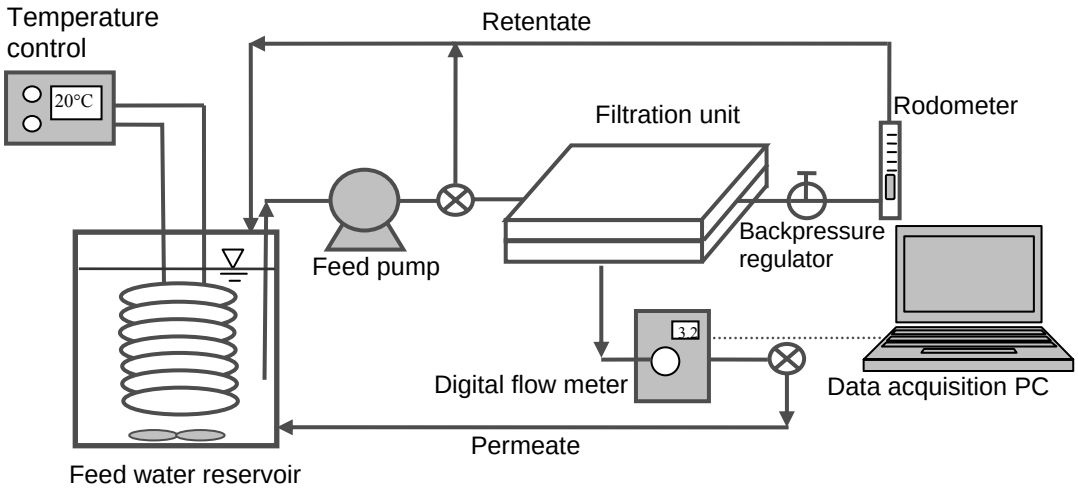

Figure 2. Schematic of the cross-flow filtration system.

Bench-Scale Membrane Fouling/Cleaning Experiments. Fouling experiments were conducted using synthetic waters containing colloids only, humic acid only or both colloids and humic acid with ionic compositions of the water varied systematically. Chemical cleaning was conducted immediately after the fouling experiments. Chemical cleaning efficiency was evaluated by measuring membrane flux of foulant-free feed water after cleaning.

Microscopic Characterization of the Fouling Layer. For every membrane filtration/chemical cleaning experiment conducted, an additional membrane filtration experiment was performed under identical experimental conditions to produce fouled membranes for microscopic characterization of the fouling layer. Each fouled membrane sample was cut into halves. One half was air dried immediately and prepared for scanning electron microscope (SEM) analysis of

the fouling layer surface. Another half of the fouled membrane sample was fractured via a cryogenic method to expose the cross-section of the fouling layer and subsequently freeze-dried and imaged with the SEM.

Principal Findings and Significance

Synergetic effect during combined fouling. Under the same solution chemistry, combined fouling caused drastically greater membrane flux decline. Figure 3 compares membrane flux decline as a function of permeate volume during colloidal fouling, organic fouling and combined fouling when SRHA and ST-XL silica colloids were used as the model organic and colloidal foulants, respectively. At any given permeate volume, the amount of organic foulant and colloidal foulant transported from the bulk phase to the membrane surface during combined fouling is equal to those during the corresponding organic fouling and colloidal fouling experiments, respectively. As shown in Figure 3, the flux decline during the combined fouling experiments are significantly higher than the simple addition of the flux decline during the organic fouling experiment and the colloidal fouling experiment, indicating synergistic effect when both colloidal and organic foulants are present in the feed solution. The synergistic effect is more prominent when the larger colloid, MP3040, was used (Figures 3(c) and 3(d)).

Effect of solution chemistry. In a previous investigation on organic fouling of NF membranes, distinctive effects of Na^{2+}, Mg^{2+} and Ca^{2+} were reported [4]. Na^{+} and Mg^{2+} only caused slight flux decline while great reduction of membrane flux was obserfed when Ca^{2+} was present in the feed solution. Li and Elimelech [4] explained the dramatic effect of Ca^{2+} on the enhanced membrane fouling rate with an inter-molecular bridging effect.

In this study, the effects of these cations were found very different in colloidal fouling and combined fouling. Membrane flux was found to be independent of ionic composition at the same total ionic strength in colloidal fouling, as demonstrated in Figure 4(a). When both colloidal foulants and organic foulants were present in the feed solution, the membrane flux decline rate was significantly higher in the presence of 1 mM Ca^{2+} or Mg^{2+} than with Na^{+} alone, while the former two resulted in the same membrane flux (see Figure 4(b)).

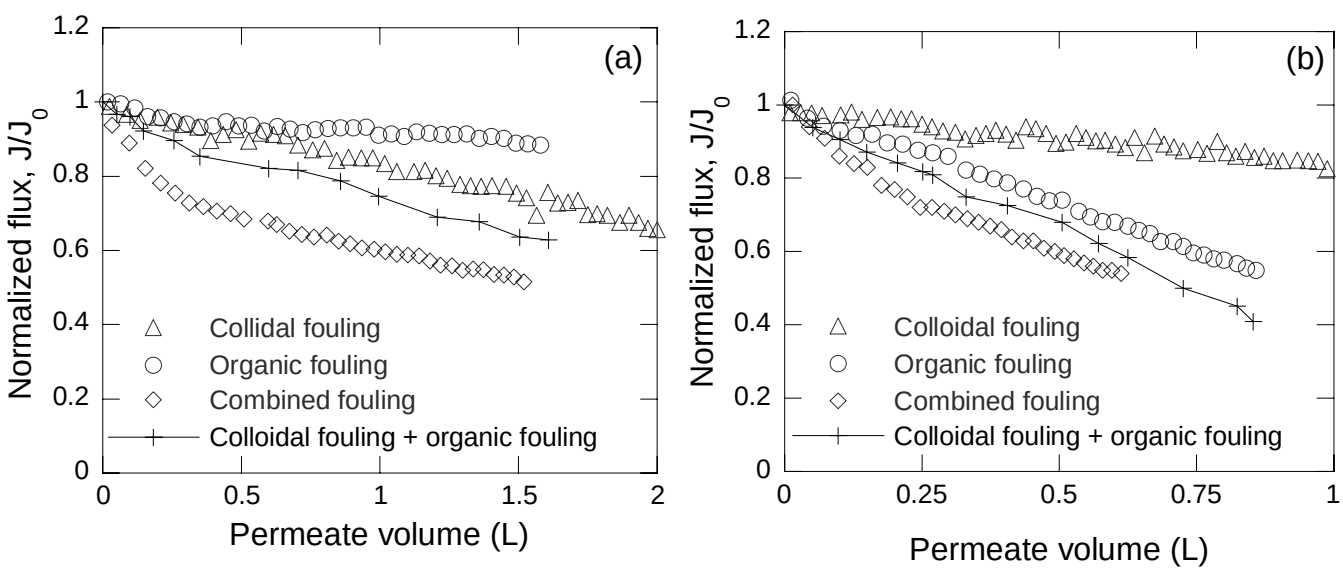

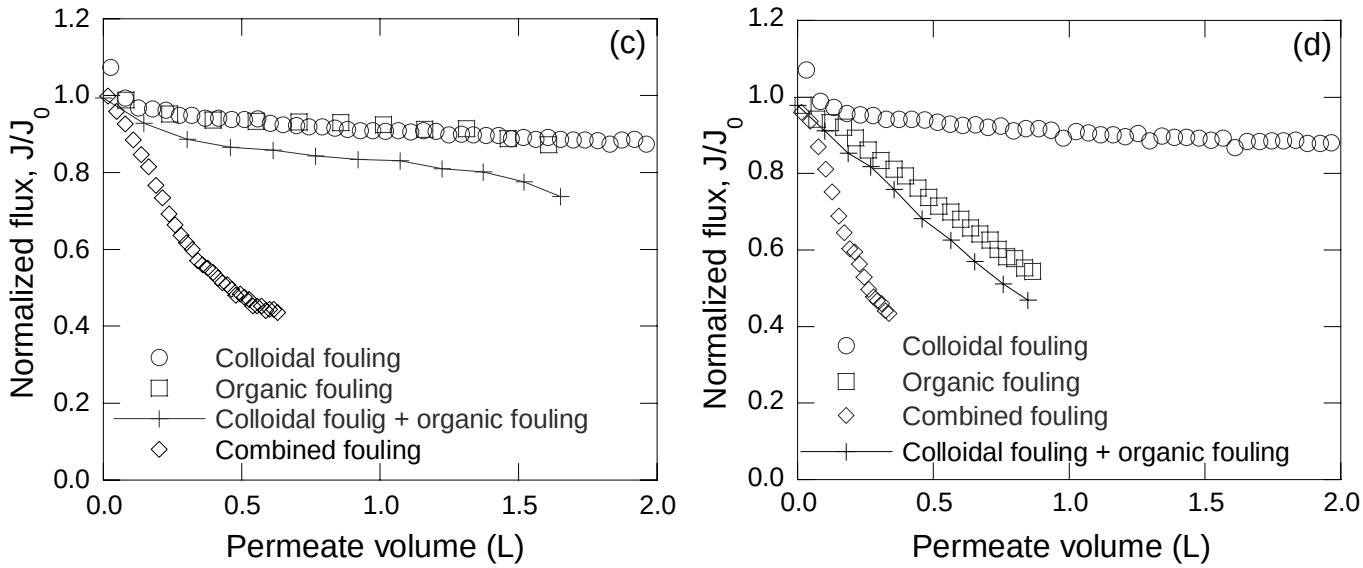

Figure 3. Synergistic effect of combined fouling. (a) Zero divalent ions with ST-XL as the colloidal foulant; (b) 1 mM Ca^{2+} with ST-XL as the colloidal foulant; (c) Zero divalent ions with MP3040 as the colloidal foulant; (d) 1 mM Ca^{2+} with MP3040 as the colloidal foulant. Total ionic strength = 10 mM, pH = 8.1, $J_0 = (1.82 \pm 0.03) \times 10^{-5}$ m/s; The organic foulant used is 20 mg/L SRHA and the colloidal foulant concentration is 100 mg/L.

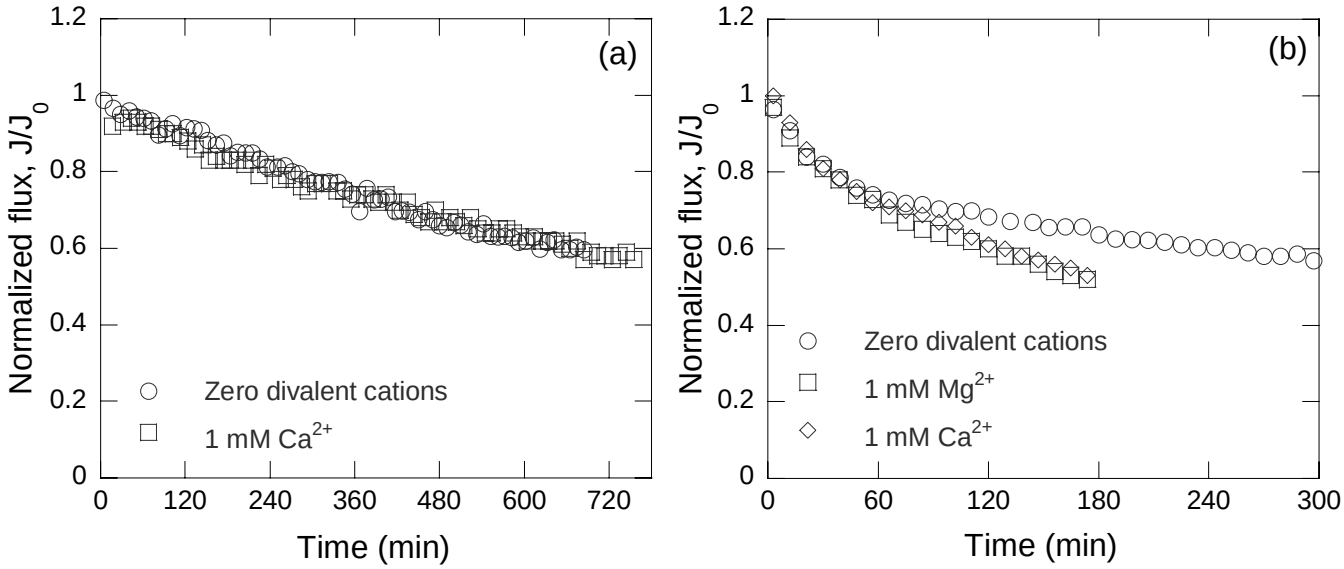

Figure 4. The effect of ionic composition on NF 270 membrane flux during (a) colloidal fouling and (b) combined fouling. Total ionic strength = 10 mM, pH = 8.1, $J_0 = (1.82 \pm 0.03) \times 10^{-5}$ m/s. The organic foulant and colloidal foulant used are 20 mg/L SRHA and 100 mg/L ST-XL, respectively.

Effect of particle size. In colloidal fouling experiments (Figure 5(a)), the small colloid, ST-XL, caused more fouling than the large colloid, MP3040. This is because of the higher specific resistance of the cake layer formed by smaller particles, as predicted by the Carman-Kozeny relationship (Eq 1), where $\hat{R}_c$ is the specific resistance of the colloidal cake layer, ε the porosity of the cake, ρ_p the density of the particles, and d_p is the particle size [5].

$$\hat{R}_c = \frac{180(1-\varepsilon)}{\rho_p d_p^2 \varepsilon^3} \qquad (1)$$

The effect of colloidal particle size is different in combined fouling experiments. In the presence of 20 mg/L SRHA, MP3040 caused significantly faster fouling rate both with and without Ca^{2+} compared to ST-XL, as shown in Figure 5(b).

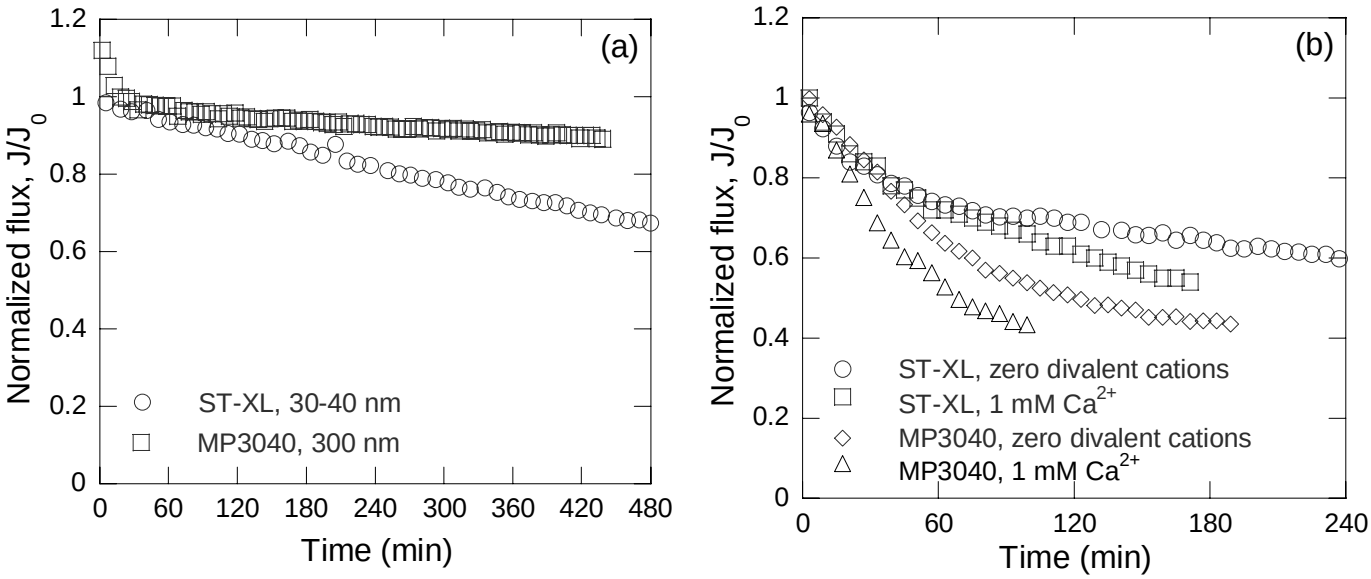

Figure 5. Effect of colloidal particle size on (a) colloidal fouling and (b) combined fouling. Total ionic strength = 10 mM, pH = 8.1, $J_0 = (1.82 \pm 0.03) \times 10^{-5}$ m/s. The SRHA concentration is 20 mg/L.

Chemical cleaning. Using the same membrane, NF270, Li and Elimelech [4] reported chemical cleaning efficiencies after fouling by humic acid in the presence of Ca^{2+}. Cleaning agents capable of removing Ca^{2+} from the Ca-humic acid association, e.g. SDS and EDTA, were found to be effective, while deionized water or NaOH solution (pH 11) was not able to achieve significant flux recovery. The formation of a dense fouling layer via intermolecular bridging by Ca^{2+} among humic acid molecules is believed responsible for the poor cleaning efficiency by deionized water and the NaOH solution.

After colloidal fouling, complete flux recovery was obtained simply by releasing the pressure and rinsing with deionized water. This is due to the repulsive force among silica colloids as well as that between the colloids and the membrane surface since both silica and the membrane surfaces are highly negatively charged in deionized water. Figure 6 compares the recovered flux after the membrane samples fouled by a feed solution containing both ST-XL and SRHA were cleaned with different cleaning solutions. Unlike membranes fouled by SRHA alone, very high flux recovery, over 90% of the initial flux, was obtained by simply cleaning with deionized water regardless of the solution condition used during fouling. The difference in chemical cleaning efficiencies of membranes after combined fouling and after organic fouling [4] clearly shows that intermolecular bridging of Ca^{2+} is not the major mechanism in combined fouling.

Effect of system configuration. Figure 7 compares the membrane flux during colloidal fouling, organic fouling and combined fouling in dead-end and cross-flow filtration. The cross-flow filtration mode showed slower membrane fouling rate in all cases due to the higher hydraulic shearing, especially in organic fouling. As observed in the dead-end filtration system, the

synergetic effect of combined fouling caused much faster flux decline than organic fouling or colloidal fouling alone. The synergetic effect is more prominent in the cross-flow mode considering the very low fouling rate caused by colloidal or organic foulant alone.

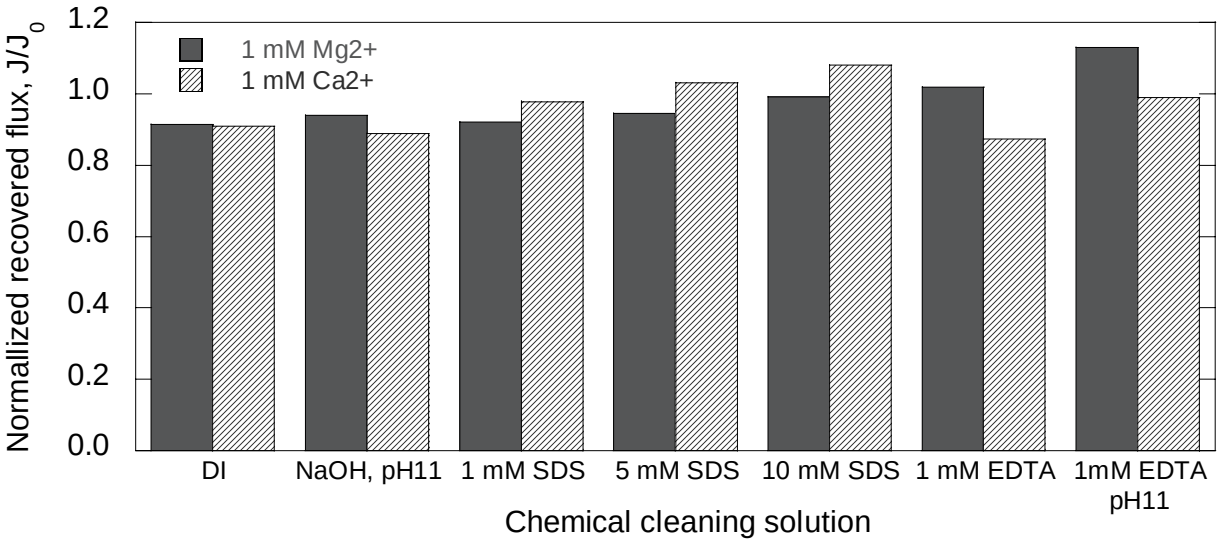

Figure 6. Chemical cleaning efficiency of various chemical cleaning solutions after combined fouling of the NF 270 membrane. Fouling experiment conditions: total ionic strength = 10 mM, pH = 8.1, $J_0 = (1.82 \pm 0.03) \times 10^{-5}$ m/s. The organic foulant and colloidal foulant used are 20 mg/L SRHA and 100 mg/L ST-XL, respectively.

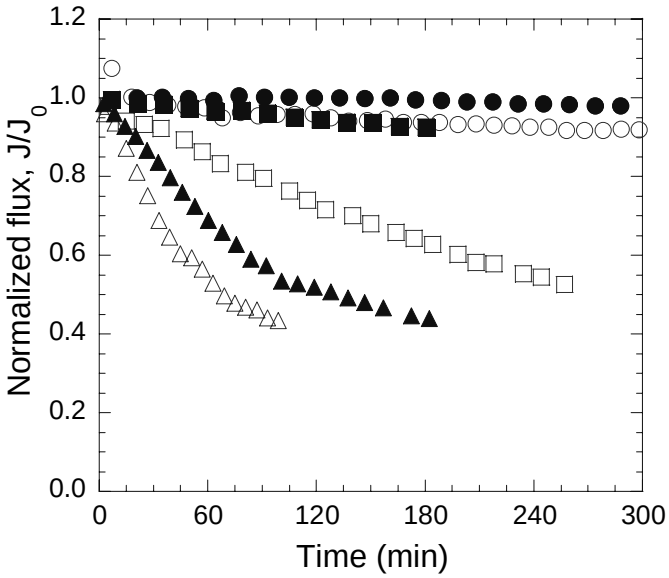

Figure 7. Comparison of membrane performance in a dead-end filtration system (open symbols) and a cross-flow filtration system (close symbols): (○) colloidal fouling; (□) organic fouling; (Δ) combined fouling. Total ionic strength = 10 mM, Ca^{2+} = 1 mM, pH = 8.1, J_0 (dead-end) = $(1.82 \pm 0.03) \times 10^{-5}$ m/s, J_0 (crossflow) = $(1.95 \pm 0.02) \times 10^{-5}$ m/s ; . The organic foulant and colloidal foulant used are 20 mg/L SRHA and 100 mg/L MP3040, respectively.

Combined fouling mechanisms. Based on the experimental results, it is proposed that the enhanced membrane flux decline is a result of hindered back diffusion of colloidal and organic foulants. Foulant accumulation rate is determined by the coupled effect of permeate flow drag force, hydraulic shearing force and the back diffusion of the foulant. The colloidal cake layer

formed on the membrane surface reduces the back diffusion rate of organic foulant molecules by forming a tortuous pathway for the back diffusion of the organic foulant. The enhanced accumulation of the organic foulant increases the viscosity in the boundary layer, which in turn lowers the back diffusion rate of the colloidal foulant as predicted by the Stokes-Einstein equation (Eq 2), resulting in faster deposition rate of the colloidal material. The high initial flux decline rate during the combined fouling experiments is the result of the enhanced accumulation rate of the organic as well as colloidal foulants.

$$D = \frac{kT}{3\pi\mu d_p} \qquad (2)$$

D = Diffusion coefficient of the suspended colloids, m^2/s;

k = Boltzmann's constant, 1.38×10^{-23} J/K;

T = Temperature, K;

μ = Viscosity, Pa·s;

d_p = Particle diameter, m;

Moreover, the heterogeneous colloidal/organic fouling layer has such a structure that the organic foulant among colloidal particles holds the colloidal particles on the membrane surface even when the pressure is released. Figure 8 shows the SEM images of the surface and cross-section of the NF270 membrane fouled by colloidal foulant alone and after combined fouling. The small number of silica colloids on the membrane surface after colloidal fouling indicates that the colloidal cake layer is held by the transmembrane pressure during the filtration process. Once the pressure is removed, the silica colloids in the cake layer are released from the membrane surface and resuspended in the bulk phase. However, when organic foulant is also present, the fouling layer is a mixture of colloidal and organic foulants consisting of multiple layers of silica colloids, indicating that the silica colloids are held on the membrane surface by the organic foulant molecules.

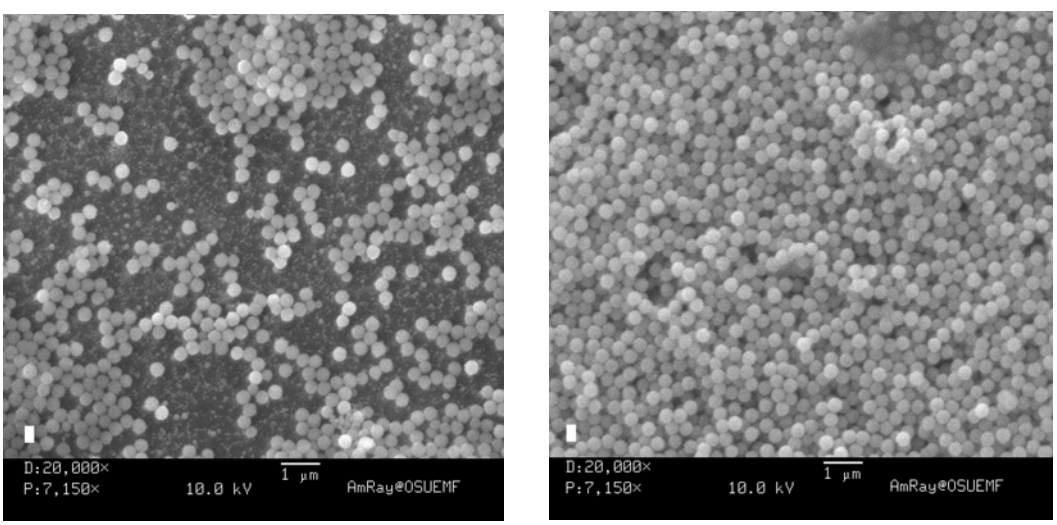

(a) (b)

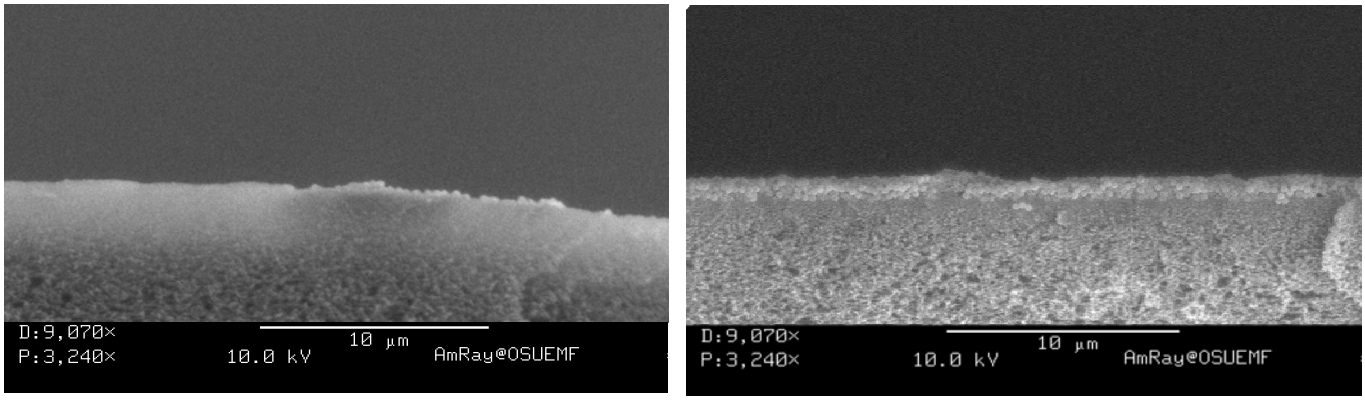

(c) (d)

Figure 8. SEM image of the fouled NF270 membrane. (a) Surface after colloidal fouling; (b) Surface after combined fouling; (c) Cross section after colloidal fouling; and (d) Cross section after combined fouling. Fouling experiment condition: total ionic strength = 10 mM, pH = 8.1, $J_0 = (1.82 \pm 0.03) \times 10^{-5}$ m/s. The organic foulant and colloidal foulant used are 20 mg/L SRHA and 100 mg/L MP3040, respectively.

Training and publications

A PhD student, Zhihua Xu, a MS student, Chaithanya Rekha Vuppala, and an undergraduate student, Chris Irvine worked on and were supported by this project. Publications and conference presentation that are based on this study are listed below.

- Journal publication

  Li, Q. and Elimelech, M. **Synergistic Effects in Combined Fouling of a Low Salt Rejection Nanofiltration Membrane by Colloidal Materials and Natural Organic Matter**. (In preparation).

- Conference presentations

  Xu, Z., and Li, Q. **Combined Fouling and Chemical Cleaning of Nanofiltration Membranes**. The PNW Section AWWA Annual Conference. Portland, Oregon, May 4-6, 2005.

  Li, Q. and Elimelech, M. **Combined Colloidal and Organic Fouling and Chemical Cleaning of Nanofiltration Membranes**. *The 15th North America Membrane Society Annual Meeting*. Honolulu, Hawaii, June 26-30, 2004.

  Li, Q. and Elimelech, M. **Combined Fouling of Nanofiltration Membranes by Colloidal Material and Natural Organic Matter and Chemical Cleaning of the Fouled Membranes**. *The 78th ACS Colloid and Surface Science Symposium.* New Haven, Connecticut, June 20-23, 2004.

Reference

Childress, A.E. and M. Elimelech, *Effect of solution chemistry on the surface charge of polymeric reverse osmosis and nanofiltration membranes.* Journal of Membrane Science, 1996. **119**(2): p. 253-268.

Elimelech, M., W.H. Chen, and J.J. Waypa, *Measuring the Zeta (Electrokinetic) Potential of Reverse-Osmosis Membranes by a Streaming Potential Analyzer.* Desalination, 1994. **95**(3): p. 269-286.

Trägårdh, G., *Membrane Cleaning.* Desalination, 1989. **71**(3): p. 325-335.

Li, Q. and M. Elimelech, *Organic fouling and chemical cleaning of nanofiltration membranes: Measurements and mechanisms.* Environmental Science & Technology, 2004. **38**(17): p. 4683-4693.

Carman, P.C., *Fundamental Principles of Industrial Filtration.* Trans. Inst. Chem. Eng., 1938. **16**: p. 168-187.